ARL-TR-7802 ● SEP 2016

US Army Research Laboratory

Joint Aircraft Survivability Program Final Test Report for the Acoustic Fire Suppression Project JASP-TR-14-05

by Adam Friedman, Brent T Mills, and Ed Habtour

NOTICES

Disclaimers

The findings in this report are not to be construed as an official Department of the Army position unless so designated by other authorized documents.

Citation of manufacturer's or trade names does not constitute an official endorsement or approval of the use thereof.

Destroy this report when it is no longer needed. Do not return it to the originator.

ARL-TR-7802 ● SEP 2016

US Army Research Laboratory

Joint Aircraft Survivability Program Final Test Report for the Acoustic Fire Suppression Project JASP-TR-14-05

by Adam Friedman, Brent T Mills, and Ed Habtour
Vehicle Technology Directorate, ARL

REPORT DOCUMENTATION PAGE

Form Approved
OMB No. 0704-0188

1. REPORT DATE *(DD-MM-YYYY)*	2. REPORT TYPE	3. DATES COVERED (From - To)
September 2016	Technical Report	2014 October–2016 April

4. TITLE AND SUBTITLE
Joint Aircraft Survivability Program Final Test Report for the Acoustic Fire Suppression Project JASP-TR-14-05

5a. CONTRACT NUMBER

5b. GRANT NUMBER

5c. PROGRAM ELEMENT NUMBER

6. AUTHOR(S)
Adam Friedman, Brent T Mills, and Ed Habtour

5d. PROJECT NUMBER

5e. TASK NUMBER

5f. WORK UNIT NUMBER

7. PERFORMING ORGANIZATION NAME(S) AND ADDRESS(ES)
US Army Research Laboratory
ATTN: RDRL-VTM
Aberdeen Proving Ground, MD 21005-5066

8. PERFORMING ORGANIZATION REPORT NUMBER
ARL-TR-7802

9. SPONSORING/MONITORING AGENCY NAME(S) AND ADDRESS(ES)
OSD/DOT&E/LFT&E
1700 Defense Pentagon
Washington, DC 20301-1700

10. SPONSOR/MONITOR'S ACRONYM(S)
OSD/DOT&E/LFT&E

11. SPONSOR/MONITOR'S REPORT NUMBER(S)
JASP-TR-14-05

12. DISTRIBUTION/AVAILABILITY STATEMENT
Approved for public release; distribution is unlimited.

13. SUPPLEMENTARY NOTES

14. ABSTRACT
The Joint Aircraft Survivability Program (JASP)-V-14-05 was a collaborative, 3-year Joint Aircraft Survivability (Joint Live Fire-Air) project to develop a lightweight, low-power, acoustic, fire-suppression system. This report documents the background, mechanisms research, and prototype development for JASP-V-14-05. We found that the strongest influence on the flame's mass flux was the magnitude of oscillatory air movement experienced by the flame. Acoustic perturbations were imposed on flames to determine acoustic extinction criterion. Using the data collected, a model was developed that characterized the acoustic conditions required to cause flame extinction. The model was based on the ratio of an acoustic Nusselt Number to the Spalding B Number of the fuel, and it was found that at the minimum speaker power required to cause extinction this ratio was a constant. Furthermore, we found that at conditions where the ratio was below this constant, a flame could still exist at conditions where the ratio was greater than or equal to this constant, flame extinction always occurred. These data were then used to design criteria for a prototype carbon nanotube (CNT) thermoacoustic speaker. Of the 3 designs fabricated, none of the CNT thermoacoustic speakers were capable of producing over 100-dB sound pressure level below 100 Hz and could not extinguish the flame. Additional research and development with CNT thermoacoustic speakers is required before the technology is suitable for acoustic flame extinction at low frequencies.

15. SUBJECT TERMS
joint aircraft survivability, JASP, JP-8, fire, fire suppression, flame extinction, JASP V-14-05

16. SECURITY CLASSIFICATION OF:			17. LIMITATION OF ABSTRACT	18. NUMBER OF PAGES	19a. NAME OF RESPONSIBLE PERSON
a. REPORT	b. ABSTRACT	c. THIS PAGE			Brent T Mills
Unclassified	Unclassified	Unclassified	UU	38	19b. TELEPHONE NUMBER (Include area code) 410-278-2468

Contents

List of Figures v

List of Tables v

Executive Summary vii

1. Introduction 1

2. Objective 1

3. Background 1

3.1 Traditional Fire Extinction 1

3.2 Interactions of Acoustics and Flames 3

3.3 Carbon Nanotube (CNT) Thermoacoustic Actuators 6

4. Test Setup 6

5. Acoustic Extinction 8

5.1 Test Procedure 8

5.2 Acoustic Extinction Results 9

5.3 Fan-Driven Extinction Results 10

5.4 Comparison of Results 11

5.5 Proposed Extinction Theory 12

5.5.1 Heuristic Framework 13

5.5.2 Proposed Extinction Criterion 14

6. Acoustic Fire Suppression Prototype 19

7. Conclusions 20

8. Limitations and Considerations 21

9. References 22

List of Symbols, Abbreviations, and Acronyms **27**

Distribution List **28**

List of Figures

Fig. 1 Burner schematic 7
Fig. 2 Testing enclosure 8
Fig. 3 Average acoustic extinction criteria (P_{Aext}) 10
Fig. 4 Average acoustic extinction criteria (U_{Aext}) 10
Fig. 5 Comparison of U_{Fext} and U_{Aext} 11
Fig. 6 Hexane flame oscillation over one period (35 Hz) 13
Fig. 7 Coefficient of variation for Θ_A' 17
Fig. 8 Calculated Θ_A' for acoustic extinction 18
Fig. 9 Thin-film CNT thermoacoustic speaker prototypes 19
Fig. 10 Sample frequency characterization of Panel A 20

List of Tables

Table 1 Summary of the acoustic flame-extinction results 9
Table 2 Summary of the acoustic flame-extinction results 11
Table 3 Comparison of averaged U_{Fext} and U_{Aext} 11
Table 4 Selected properties of fuels and gases 15
Table 5 Selected properties of air for different fuels 16
Table 6 Calculated fuel properties 16
Table 7 Analysis of hypo and hyper critical extinction conditions 18

INTENTIONALLY LEFT BLANK.

Executive Summary

The Joint Aircraft Survivability Program (JASP)-V-14-05 was a collaborative, 3-year project to develop a lightweight, low-power, acoustic, fire-suppression system. The US Army Research Laboratory's Vehicle Technology Directorate (ARL-VTD) with the University of Maryland's Fire Protection Department investigated the mechanisms of acoustic fire extinction to characterize the design requirements for the prototype system. The NanoTech Institute from the University of Texas at Dallas designed and fabricated the prototype system. This report documents the background, mechanisms research, and prototype development for JASP-V-14-05.

A study of acoustically driven extinction was carried out using the alkanes and JP-8. Samples were ignited and then subjected to acoustic perturbations at various frequencies and speaker powers until the minimum speaker power was found that could cause 3 consecutive flame extinctions. The root-mean-square (rms) acoustic pressure and air speed were measured during each trial and, along with frequency, these measurements were used to characterize the acoustic conditions. The minimum fan-driven flows required to cause extinction for each fuel was also evaluated. Analysis of the data showed that the fan-driven air speed required to cause extinction of each fuel increased with the fuel's heat of combustion per unit mole, and that this trend was consistent with extinction strain rate theory. Using acoustics the rms air speed at extinction was seen to decrease, which indicated that flame elongation was not the cause of extinction using acoustics. High-speed video showed that during acoustic excitation, the flame would become detached, forced away from the fuel bed, and then returned and reattached until the next cycle. It was theorized that during this displacement phase the fuel bed experienced convective cooling, and that this eventually caused the fuel's mass flux to fall below the critical amount needed to sustain the flame. This hypothesis was consistent with other theories to explain the acoustically driven extinction of droplet flames. To explore this hypothesis, the flame was conceptualized in a simple model between flame and fuel source. In this model, the Spalding B Number was used to characterize the interplay between the flame and fuel, and a Nusselt Number was used to characterize the convective cooling of the fuel bed. Mathematical expressions were then developed for each of the numbers and they were evaluated using values reported in the literature and conditions measured during the experiment. It was found that at the minimum speaker power required to cause extinction, the ratio of the Nusselt Number to B Number was a constant for all fuels at all frequencies tested. It was found that when this ratio was below the constant, the flame continued to burn. If the ratio was greater than or equal to the constant, then flame extinction

occurred. It was therefore asserted that this constant constituted a boundary between regions of flammability and flame extinction.

These data were then used the design criteria for a prototype carbon nanotube (CNT) thermoacoustic speaker. Of the 3 designed and fabricated, none of the CNT thermoacoustic speakers were capable of producing over 100-dB sound pressure level (SPL) below 100 Hz. As a result none of the CNT thermoacoustic speakers were sufficient for acoustic fire-extinction. Additional research and development with CNT thermoacoustic speakers is required before the technology is suitable for acoustic flame extinction at low frequencies.

1. Introduction

Since the early 1900s halon has been used to effectively extinguish fires.[1] Starting in the 1960s halon began to see widespread use in the US Department of Defense (DOD), and it quickly become one of the primary fire and explosion extinguishing agents employed.[2] Due to the ozone depleting properties of halon, the United States became a signatory to the Montreal Protocol in 1987, which effectively ended the production of halon worldwide.[3] To meet its present needs for halon, the DOD maintains a reserve that is supplemented with product acquired from decommissioned systems. With no new halon available, finding a suitable halon replacement technology has become an active area of research for the DOD.[2]

The Joint Aircraft Survivability Program (JASP)-V-14-05 was a collaborative, 3-year Joint Aircraft Survivability (Joint Live Fire [JLF]-Air) project to develop a lightweight, low-power, acoustic, fire-suppression system. The US Army Research Laboratory's Vehicle Technology Directorate (ARL-VTD) with the University of Maryland's Fire Protection Department investigated the mechanisms of acoustic fire extinction to characterize the design requirements for the prototype system. The NanoTech Institute from the University of Texas at Dallas (UTD) designed and fabricated the prototype system. This report documents the background, mechanisms research, and prototype development for JASP-V-14-05.

2. Objective

To design and demonstrate a lightweight, low-power, acoustic, fire-suppression system using carbon nanostructure materials.

3. Background

This section provides a brief background on traditional fire-extinction mechanisms, the interactions of acoustics and flames, and carbon nanotube (CNT) thermoacoustic actuators.

3.1 Traditional Fire Extinction

Diffusion flames, such as pool fires, are flames in which the oxidizer combines with the fuel by diffusion (the net movement of molecules from a region of high concentration to a region of lower concentration). Diffusion flame extinction occurs when the heat released during combustion can no longer maintain a temperature that will sustain chemical kinetics due to heat losses from the flame.[4] It has been proposed that for every flame there exists a critical temperature, below which flame

extinction will occur.[5] For example, introduction of a diluent, such as liquid water or a dry-chemical agent, reduces the oxidizer's concentration, thereby reducing the chemical reaction and heat release rates while absorbing energy (i.e., heat) from the flame and fuel source. This cools the fuel source and inhibits pyrolysis while also creating significant heat losses from the flame. Additional agents and chemicals may also bind with free radicals interrupting the chemical reaction processes for combustion further lowering temperatures in the flames and retarding chemical kinetics.[6,7]

However, chemical kinetics alone does not fully explain extinction phenomenon.[8] Closely coupled with kinetics are heat and mass transport processes, which are needed to create a combustion environment. The amount of strain experienced by the flame is of particular interest when considering transport processes. For diffusion flame, if conceptualized in the context of a reactive flow, strain is considered as a measure of the rate of deformation in the flow.[9] As strain in the reactant flows increases, the residence time of the reactants decreases.[10] This in turn has the effect of lowering both the reaction and heat release rates.[10,11] For diffusion flame, if conceptualized in the context of a "cellular" entity with a surface, strain is considered as elongation, a measure of curvature in the flame surface. As the flame elongates, the symmetry between the fuel and oxidizer sides of the flame decreases, and this causes imbalances in heat and mass fluxes on either side of the flame.[12] For steady diffusion flames, increased flame elongation results in increased heat losses from both sides of the reaction zone.[13] For unsteady diffusion flames, elongation is considered as the proportional rate of change in the flame surface area in respect to time.[14] Katta et al. showed that the effects of elongation on the unsteady flame also created transport imbalances. In their study of an unsteady opposing jet flames, they found that as the flame elongates, the amount of reactant that was able to enter the reaction zone also increased. The net effect was that while the heat release rate increased, there was also an increase in the amount of products from incomplete combustion. These products acted as a heat sink within the flames and lowered the flame temperature.[15]

Flame elongation has become a commonly used criterion for predicting fame extinction.[5,8,10,11,16–18] Underlying this, is the understanding that flame elongation enhances transport processes, which in turn competes with combustion reaction chemical kinetics. Using an Asymptotic Energy Analysis, Lecoustre et al. showed that as flame stretch increased, the temperature required to sustain a diffusion flames also increased. Since the effects of transport processes and chemical kinetics though are so closely coupled, it is desirable to represent them in relationship to each other as commonly done through the Damköholer Number. The Damköholer Number (*Da*) of a flame is generally define as the ratio of a characteristic mixing

(transport or residence) time (τ_{mix}) to a characteristic chemistry time (τ_{chem}).[5,16–19] Mathematically, this is expressed as $Da = \frac{\tau_{mix}}{\tau_{chem}}$. As rates are inversely proportional to time, and it is sometimes useful to express the Damköholer Number as the ratio of the reaction rate to the mixing rate. For large Damköholer Numbers, we can expect the effects of slow-transport processes to dominate and for flame chemistry to occur at a faster rate. As the Damköholer Number decreases, the effects of increased transport rates and slower chemical kinetics begins to dominate until the system becomes nonreactive.[19] Therefore, for every flame there exists a critical Damköholer Number, below which flames extinction will occur.[5,17,20]

3.2 Interactions of Acoustics and Flames

The interaction of acoustic waves and flames has been a field of study as early as the 1960s. The primary focus of early research was the effects of acoustics on droplet burning in turbine engines and combustion chambers.[5,21–23] The results of this continued research has shown that acoustics do influence droplet combustion by altering the rates of heat and mass transfer.[23] Of particular interest are the instabilities that form within a combustion chamber.[5] These instabilities can often lead to combustion inefficiencies and damage to the chamber.[5,24] The causes of these phenomena are due to disturbances in the reaction flow field.[25]

Although acoustics can lead to inefficiencies during droplet combustion, they can also be used to enhance combustion. During spray processes, fuel droplets often break up into smaller subdroplets, and some of these subdroplets may be inhomogeneous with lower boiling temperatures. Rapid boiling of these subdroplets can create microexplosions that cause further droplet breakup and leads to instabilities within the reaction chamber. Miglani et al. found that the application of acoustics in the narrow bandwidth of 80 to 120 Hz could stabilize the fuel droplets and reduce the number of subdroplets formed.[26]

Acoustics can also be used to modulate the burning rate and combustion chemistry of fuel droplets. Sevilla-Esparza et al.[23] studied droplet combustion of ethanol, methanol, JP-8, and synthetic fuel at various frequencies within a standing wave. Their results showed that the burning rate of each fuel was sensitive to both frequency and phase angle, and they attributed this sensitivity to the deflection angle of the droplet within the wave. They found that at low-acoustic frequency there was a strong coupling between the relative $OH*$ concentration and the acoustic pressure. As the acoustic frequency was increased, the strength of this coupling was seen to diminish. They concluded that the coupling was attributable to the magnitude of velocity perturbation experienced by the droplet, which decreased as the acoustic frequency increased.[23]

Within the context of this research there have also been investigations into acoustically driven extinction of droplet flames. McKinney and Dunn-Rankin[22] studied this phenomenon using a streaming flow of methanol droplets. They found that at the same frequency, the acoustic pressure required to cause extinction increased with droplet size. They also found that for droplets of the same size, the acoustic pressure required to cause extinction increased with frequency. The authors determined that extinction occurred when the flame was displaced far enough from the droplet that evaporation was shut down. Key to their finds was the fact that the magnitude of displacement had to be at least the radius of the droplet.[22]

More recently, there has been a growing body of research on the interaction acoustics with both premixed and diffusion flames using gaseous fuel sources.[20,21,27–33] The breadth of this research has included a myriad of topics such as pollutant reduction,[31] combustion instabilities,[33] and even acoustic flame extinction.[20,21,30] Key to this research has been the need to understand the effects of an oscillatory strain rate on flames. Of particular interest are the effects when a flame is near its extinction limit where flames show an increased sensitivity to acoustic excitations.[27]

The response of a flame to acoustic excitations can be classified as either linear or nonlinear in respect to the excitation frequency.[32] Kim and Williams[20] studied linear responses and acoustic extinction criterion by applying a theoretical analysis to a counter-flow diffusion flame. They considered the effects of acoustic perturbations on the reactive layer in the frequency range of 103–104 Hz, which is on the same order of magnitude as the extinction strain rate for most hydrocarbon fuels. To evaluate their results, the authors used a Rayleigh criterion, which states that acoustic instabilities become greatest when the acoustic pressure and flame's heat release rate are in phase.[34] The results of their analysis showed that linear responses in the flame's position, heat release rate, and the Damköholer Number were caused by oscillations in the reaction sheet and by oscillations in the magnitude of field variables (e.g., pressure, velocity, density) in the transport zone. Near the flame's extinction limit the oscillations in the reaction sheet were dominant and produced the most dramatic effect. When closer to equilibrium conditions, the oscillations in the field variables were dominant, although these produced much less dramatic effects.[20]

Wang et al. studied the nonlinear effects of acoustics on the puffing frequency and flame height of a buoyant diffusion methane flame. Their results showed that while acoustics produced effects over the entire frequency range tested, the effects were particularly pronounced in the range of 6 to 20 Hz. Within this range, they found that the puffing frequency of the flame was half the excitation frequency, which they attributed to sequential bulges in the flame's natural puffing cycle being

merged into one. At higher frequencies, they found there was a "doubling" effect on the flame's puffing, which was attributed to breakdowns in the flow structures occurring at a faster rate.[29] Complementing the work of Wang et al.[29] was a study by Chen et al.,[32] who also examined the effects of acoustics on a buoyant diffusion flame. It was noted that the most dramatic effects on the flame height occurred at the lowest frequency, and that at the highest frequency there was a nonlinear response in the flame's flickering frequency.[32]

Additionally, there have been several studies that explored acoustic extinction for gaseous fueled flames.[20,21,30,35] Although Kim and Williams did identify acoustic extinction criteria in their theoretical work, their results only applied to oscillations of the flames reaction zone and its effects on flame chemistry.[20] Other authors have examined the phenomenon for flame in the context of a buoyant flow field. For example, Hardalupas and Selbach[30] studied acoustic extinction for a methane flame and Whiteside[21] studied the phenomenon for methane along with several other gaseous fuels.

Hardalupas and Selbach[30] found that at certain frequencies the acoustic perturbations could cause a lifted flame to reattach. They attributed this phenomenon to the creation of vortex rings by the waves and the impulses on the flames shed from the flow. They also explored flame extinction at 200 and 350 Hz, and concluded that the mechanism of flame extinction was blow-off. While the work of Wang[29] and Chen et al.[32] indicated that the flame's response was more sensitive to acoustic frequency than amplitude, Hardalupas and Selbach[30] concluded that it was the acoustic amplitude, which caused the largest movement of air, has the strongest effect.

Whiteside[21] looked specifically at acoustic flame extinction from a burner using methane, ethanol, hexane, and heptane. In contrast to the work of other authors, Whiteside used acoustics that propagated in a transverse direction to the flame. Whiteside found that as the molar mass of the fuel increased, so too did the acoustic pressure required to cause flame extinction. However, the extinction pressure for each fuel was independent of the burner's cross-sectional area. The author concluded that there was a minimum acoustic velocity required to cause extinction for each fuel, and that acoustic extinction could be achieved at any frequency provided the acoustic pressure was high enough to achieve that velocity. Whiteside also concluded that blow-off alone did not fully explain the extinction mechanism, since the flame could exist in a lifted state for short periods.[21]

3.3 Carbon Nanotube (CNT) Thermoacoustic Actuators

CNT films are parallel-aligned arrays of conductive CNTs that can be semitransparent and flexible. When an oscillating electrical current is applied to thin-film CNTs, sound is produced. Unlike traditional coil speakers that produce sound through mechanical vibration, thin-film CNTs are thermoacoustic actuators. Acoustic sound is a pressure wave that propagates in an adiabatic process. Therefore, as the wave propagates, the pressure oscillates and so does temperature. In the case of an alternating current applied to a thin-film CNT, the thin-film CNT is heated (due to resistivity in the CNT) during the positive and negative half-cycles of the current. This produces surface temperature oscillations at twice the frequency of the applied current. The periodic heating produces temperature "waves" that are propagated into the surrounding medium. The thermal expansion and contraction of the medium induces a corresponding pressure expansion and contraction in the medium producing sound. The amplitude of the resulting sound waves are a function of the heat capacity of the thin-film CNT, the frequency and amplitude of the electric current, and the physical properties of the surrounding medium. This enables CNT films to generate sound over a wide frequency (1–105 Hz).[36] However, at lower frequencies, the sound generation efficiency is significantly low. Since the sound pressure level (SPL) produced by CNT films is a function of the surrounding medium, the performance and efficiency of thin-film CNT thermoacoustic speakers can be modified by encapsulating the film in different mediums. Encapsulation of the CNT reduces the thermoacoustic speakers' sensitivity to the environment while increasing low-frequency performance. Furthermore encapsulation using rigid metal vibrating plats creates a resonant device that enhances performance at a specific frequency. However, heat dissipation of the interior volume restricts the power density of the speaker.[37,38,39]

4. Test Setup

A testing apparatus was designed that facilitated the study of a laminar flame experiencing acoustic perturbation. The primary objective of the design was to create a line-flame that approximated a flame sheet, which could interact with a planar acoustic wave front simultaneously across the flame's entire surface. Other key design features included the minimization of the effects from radiative heat feedback into the fuel and errant air flows around the flame. The apparatus consisted of 3 main components: an acoustic source, burner, and testing enclosure.

For the experimental investigation of the extinction mechanism, the acoustic source was an Infinity Reference 860W, 0.254-m subwoofer mounted inside a 3.05-m collimator to create a planer acoustic wave front at the burner. The subwoofer and

collimator were to be replaced with the prototype CNT thermoacoustic actuators. However, issues with the prototype CNT thermoacoustic actuators prevented acoustic flame-extinction testing with the prototypes.

The burner, Fig. 1, was constructed from steel sheet metal, and welded at the component interfaces. The burner consisted of 3 main components: support rails, a base plate, and a lid. Sandwiched between the lid and the base plate were insulation, the wick, and 2 sheets of borosilicate glass. The material used for both the wick and insulation surrounding the wick was Kaowool PM.

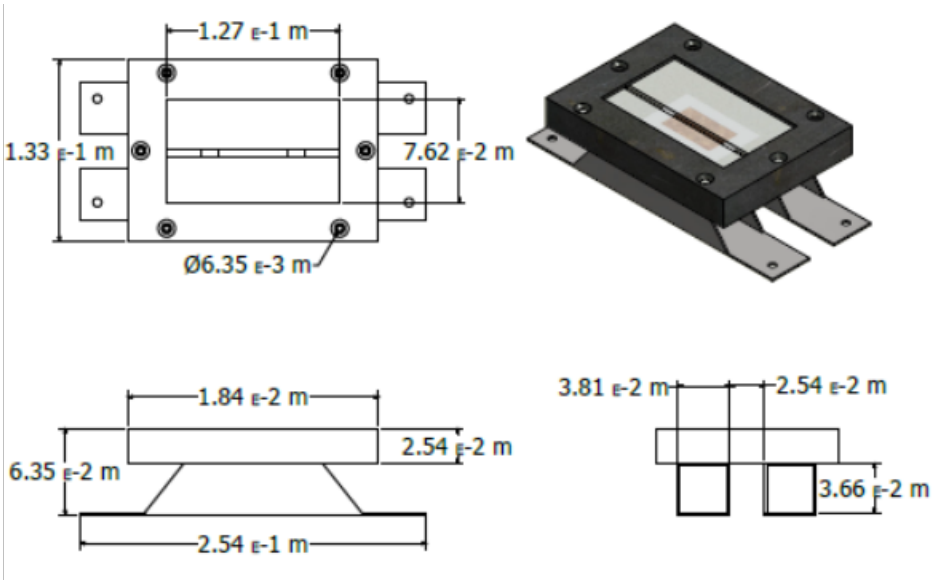

Fig. 1 Burner schematic

The testing enclosure created a space where an open flame could burn safely while simultaneously reducing the effects of errant air flows on the flame. The enclosure was built on an optical steel breadboard measuring 0.762 m × 0.762 m × 0.0635 m. The surface of the board had a grid of screw holes spaced on 1-inch squares that could accommodate 1/4−20 threading. Erected on the corners of the board were vertical metal supports. The tops of the vertical supports were connected with horizontal supports, creating a rectangular enclosure measuring 0.762 m × 0.762 m × 0.635 m. A fine steel mesh screen was then placed over the faces of the enclosure. The burner was placed within the enclosure so that the flame base would be on the center-line axis of the acoustic source. Figure 2 shows the testing enclosure as it was set up for the experimental investigation of the extinction mechanism.

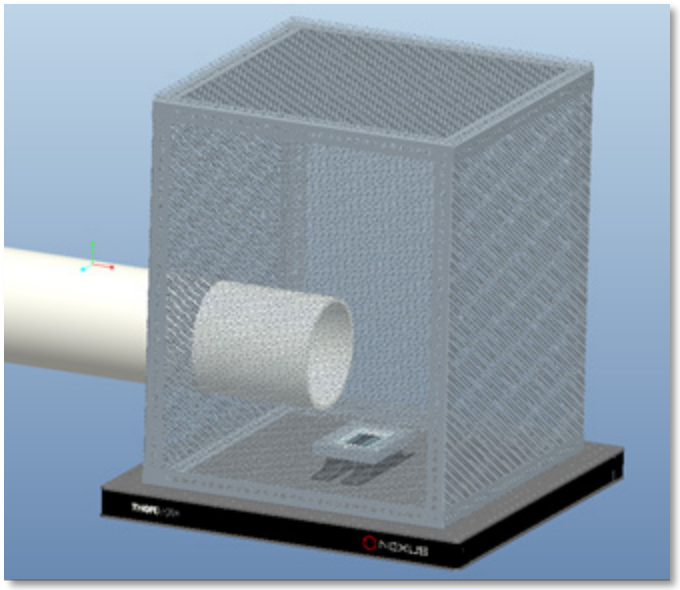

Fig. 2 Testing enclosure

Instrumentation and data acquisition were limited to methods that did not directly interact with the flame. Measurements of acoustic pressure were made using a model MPA 231 integrated constant current power microphone, manufactured by the BSWA Technology Company. The microphone was connected by BNC cable to a signal conditioner, which was then connected to a model TDS 2004B Tektronix Digital Oscilloscope. Anemometry readings were made using a model 407123 Extec Hot Wire Anemometer. Time-resolved mass readings were made using a model MS4002S Mettler Toledo Precision Balance.

5. Acoustic Extinction

This section documents the test procedure, test results, and conclusions for the 212 acoustic extinction tests conducted to investigate the mechanism of acoustic fire suppression. For comparison, 48 fan-driven extinction tests were also conducted.

5.1 Test Procedure

Laminar diffusion sheet flames fueled by n-pentane, n-hexane, n-heptane, n-octane, and JP-8 aviation fuel were subjected to sinusoidal (30 to 50 Hz) acoustic-perturbations to determine the acoustic extinction criteria. For each test, the flame was allowed to burn unperturbed until it reached a height of approximately 0.02 m. The speaker was then activated to determine if acoustically driven extinction could be achieved. Immediately after the flame was extinguished, the root mean square (rms) acoustic pressure and acoustic air speed were measured. The conditions

required to cause an acoustic extinction of a particular fuel at a particular frequency (ω) were determined by reducing the speaker power to the lowest pressure condition that could cause 3 consecutive extinction events within 10 s of speaker activation.

Similarly, laminar diffusion sheet flames fueled by n-pentane, n-hexane, n-heptane, n-octane, and JP-8 aviation fuel were subject to a fan-driven flow to determine the minimum fan-driven airspeed extinction criteria. For each test, the flame was allowed to burn unperturbed until it reached a height of approximately 0.02 m. The fan was then activated to determine if fan-driven extinction could be achieved. Immediately after the flame was extinguished, the air speed was measured. The conditions required to cause an extinction of a particular fuel were determined by reducing the fan power to the lowest airspeed condition that could cause 3 consecutive extinction events within 10 s of fan activation.

5.2 Acoustic Extinction Results

Table 1 summarizes the average rms acoustic pressure (P_{Aext}) and air speed (U_{Aext}) for the minimum power setting that could cause 3 consecutive extinction events within 10 s of speaker activation.

Table 1 Summary of the acoustic flame-extinction results

Fuel	ω (Hz)	P_{Aext} (Pa)	U_{Aext} (m/s)
Pentane	30	16.2	0.71
	35	22.2	0.86
	40	35.5	0.95
Hexane	30	14.6	0.65
	35	19.5	0.75
	40	27.0	0.68
	45	28.4	0.86
Heptane	30	13.7	0.58
	35	15.9	0.60
	40	26.6	0.72
	45	25.5	0.72
	50	29.9	0.74
Octane	30	14.7	0.58
	35	16.6	0.60
	40	25.3	0.62
	45	22.2	0.64
JP-8	30	16.1	0.55
	35	24.3	0.57
	40	23.2	0.59
	45	20.6	0.66

The extinction criteria for each fuel species can be represented as a delineating boundary between conditions where a flame can and cannot exist. In Figs. 3 and 4, flame extinction occurs at the area above the delineating criteria, at conditions below the line the flame continues to burn.

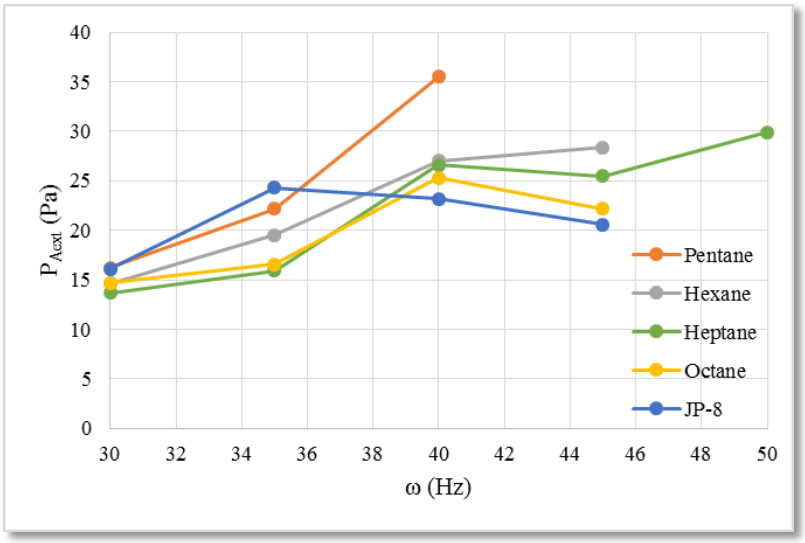

Fig. 3 Average acoustic extinction criteria (P_{Aext})

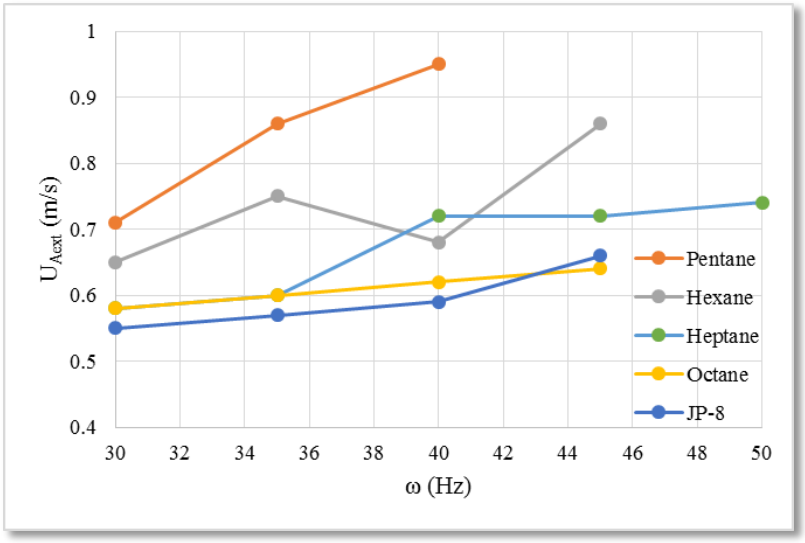

Fig. 4 Average acoustic extinction criteria (U_{Aext})

5.3 Fan-Driven Extinction Results

Table 2 summarizes the average bulk air speed (U_{Fext}) for the minimum power setting that could cause 3 consecutive extinction events within 10 s of fan activation.

Table 2 Summary of the acoustic flame-extinction results

Fuel	U_{Fext} (m/s)
Pentane	1.55
Hexane	1.58
Heptane	1.89
Octane	1.96
JP-8	2.03

5.4 Comparison of Results

When comparing the values of U_{Fext} and U_{Aext} 2 observations become apparent. First, U_{Fext} is 2 to 3 times greater than the average U_{Aext}, Table 3. Second, the general "ordering" of the fuels is reversed. For fan-driven extinctions, U_{Fext} increases with the fuel's molar mass (M) and the heat of combustion per unit mole (ΔH_c), while for acoustic extinctions, U_{Aext} decrease with M and ΔH_c, Fig. 5.

Table 3 Comparison of averaged U_{Fext} and U_{Aext}

Fuel	U_{Aext} (m/s)	U_{Fext} (m/s)	U_{Fext}/U_{Aext}	M (kg/mol)	ΔH_c (MJ/mol)
Pentane	0.84	1.55	1.84	0.0722	3.27
Hexane	0.73	1.58	2.16	0.0861	3.89
Heptane	0.67	1.89	2.82	0.1002	4.50
Octane	0.61	1.96	3.21	0.1142	5.12
JP-8	0.59	2.03	3.44	0.1533	6.56

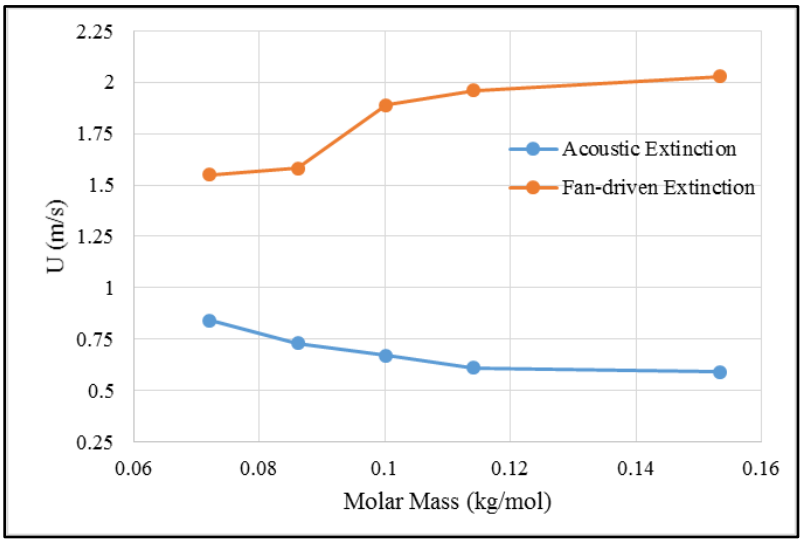

Fig. 5 Comparison of U_{Fext} and U_{Aext}

5.5 Proposed Extinction Theory

Using a "Damköholer" analysis, it has been shown that flame stretch can be a primary cause of flame extinction.[17] Flame elongation is caused by hydrodynamic strain in the flow of the oxidizer and fuel, and by localized changes in flame speed due to variations in temperature and species concentrations.[40] Except for cases where the turbulent length scales of the flow are smaller than the flame thickness, it is the hydrodynamic effects that have the strongest influence on flame elongation in laminar flames.[4]

The fan-driven extinction experiments were similar to flames in a forced flow over a stagnant fuel film, which were studied by Emmons.[41] In his analysis, Emmons showed that the flame existed in the boundary layer of the flow, and that it separated the region of cooler air from the fuel bed. As the free-stream velocity of the flow increased, the strain rate of the flow increased, the boundary layer thickness decreased, and the flame was forced closer to the fuel. Extinction occurred when the free-stream velocity and corresponding strain rate became so great, that chemical kinetics could not compete with the mixing rate of the reactants, and the Damköholer value dropped below a critical value. However, so long as combustion chemistry was occurring, the flame existed within the boundary layer of the flow.[41,42]

Won et al. showed that the extinction strain rate (a_E) for diffusion flames fueled by large hydrocarbons scales as[8]

$$a_E \propto [D_F \, Y_{F,-\infty} \, \Delta H_c] \, [\text{Kinetic Term}], \qquad (1)$$

where D_F is the diffusivity of the fuel into air and $Y_{F,-\infty}$ is the fuel mass fraction on the fuel side of the reaction zone. For the combustion of an alkane though, the number of moles of the heavier species in the mixture (e.g., CO_2 and N_2) all scale approximately with the number of carbon atoms in the fuel. In addition, the fuel's molar mass also scales roughly with the number of carbon atoms. It can be expected, therefore, that Y_F is roughly constant for all the fuels tested. In addition, values of D_F and the kinetic term should all be approximately the same when compared among the fuels. It can then be concluded that as values of ΔH_c for the fuels tested increased, the speed of the flow required to cause extinction should also have increased.

Examining the fan data, U_{Fext} does increase with ΔH_c, as expected. In contrast though, values of U_{Aext} are seen to decrease with ΔH_c. When this observation is coupled with the fact that U_{Aext} is significantly less than U_{Fext}, it suggests that flame elongation was not the cause of extinction in the acoustic experiments, and that an alternate mechanism needs to be found.

5.5.1 Heuristic Framework

Re-examining the Figs. 3 and 4, there is a positive correlation between ω with P_{Aext} and U_{Aext}. The amount of scatter in P_{Aext} is greater than in U_{Aext}. This suggests that the acoustic extinctions were more closely linked to U_A than P_A. Since we are assuming that flame elongation was not the cause of extinction, it might be reasonable to conclude that convective cooling of the wick was a cause. To understand how this process might work, conceptualize the combustion process in a simplistic flame model: fuel enters the flame region, reacts with the oxidizer, releases heat, a portion of that energy is fed back into fuel source, which drives more fuel into the flame region. In this model, the propensity of the fuel to maintain this cycle is best described by the Spalding B Number, and a large disruption to this cycle would cause flame extinction.

Examining Fig. 6, as the acoustic wave propagates over the flame holder it temporarily displaces the flame from the region above the wick. In contrast to the fan-driven flows, a boundary layer never has time to fully form in the acoustic scenario. This means that the flame is not confined to the region directly above the fuel, and that the fuel bed can be exposed directly to cool air. It can then be assumed that during the flame's displacement period, not only is the amount of heat into the wick inhibited, but that the exposed wick also experiences convective cooling from the acoustic flow. From stagnant layer theory, as the heat flux from the flame into the fuel bed decreases, so too will the fuel's mass flux.[16] Furthermore, according to the fire point theory described by Rashbash, there is a critical mass flux for any given fuel below which total flame extinction will occur.[43,44] It is reasonable to conclude that convective cooling of the fuel bed during the flame's displacement was creating conditions where fuel's mass flux is less than the critical mass flux. Assuming this is true, a local Nusselt Number could be used to characterize the magnitude of this cooling.

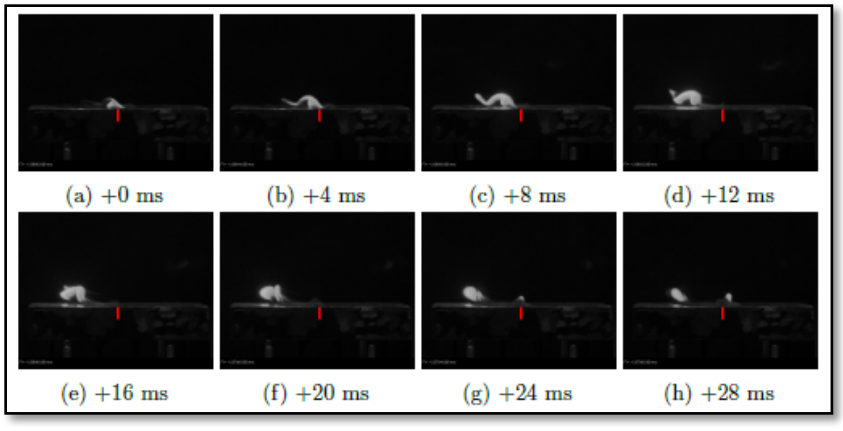

Fig. 6 Hexane flame oscillation over one period (35 Hz)

5.5.2 Proposed Extinction Criterion

In the proposed model, the B-Mass Transfer Number characterizes the fuel's ability to maintain the flame-fuel cycle, and the Nusselt Number characterizes the amount of disruption to this cycle. A ratio of these 2 nondimensional numbers might then constitute a criterion by which acoustic extinctions can be predicted. For consistency with the boundary in Figs. 3 and 4, it would be useful to structure this ratio so that larger values correspond with flame extinction, while smaller values correspond with flame residence. It is, therefore, proposed that the ratio of Nu_ξ to B at the point acoustic extinction was achieved is a constant, and that it that forms a boundary between conditions where the flame can and cannot exist. This ratio is designated Θ_A, as shown in Eq. 2.

$$\Theta_A = \frac{Nu_\xi}{B}, \tag{2}$$

where expressions for Nu_ξ and B are defined in the following sections.

5.5.2.1 B-Mass Transfer Number

In a study of ethanol and heptane pool fires of various areas with varying crosswinds, Hu et al. [45] found that the ratio of radiation absorbed by the fuel to the heat needed for vaporization (χ_a) decreased as the fuel area decreased and the crosswind increased. For their smallest heptane pool fire, which had an area of 10 cm^2, they found $\chi_a = 0.26$ with no crosswind and $\chi_a = 0.10$ with a cross flow of 0.7 m/s. In the experiments for this study the burner area was 2.5 cm^2 and $U_A = 0.68$ m/s. Although the setup and testing conditions for this study were not perfectly analogous to Hu's, it can be assumed, based on their results and general trends seen in their data that the flames in this study were driven primarily by convective heat transfer. With this assumption then, Quintiere gives the B-Mass Transfer Number as the following:[17]

$$B = \frac{Y_{O_2,\infty}\,(\Delta h_c/r) - c_{p,air}(T_b - T_\infty)}{L}, \tag{3}$$

where it is assumed that $Y_{O_2,\infty} = 0.233$ and $T_\infty = 298$ K.

For the alkanes tested and certain gases of interest, data on the following parameters was obtained from the National Institute of Standards and Technology (NIST) Chemistry WebBook,[46] and the data are reproduced in Table 4: molar mass (M); liquid specific heat at 300 K ($c_{p,\,liq}$); liquid heat of formation ($\Delta h_{f;liq}$); gaseous heat of formation ($\Delta h_{f,gas}$); heat of vaporization (h_v); and boiling temperature at 1 atm (T_b).

Table 4 Selected properties of fuels and gases

Species	M (kg/mol)	$c_{p,liq}$ (kJ/kg·K)	$\Delta h°_{f,liq}$ (MJ/kg)	$\Delta h°_{f,gas}$ (MJ/kg)	Δh_{vap} (MJ/kg)	T_b (K)
Pentane	0.07215	2.317	2.405	2.035	0.3673	309.2
Hexane	0.08612	2.268	2.306	1.940	0.3597	341.9
Heptane	0.1002	2.241	2.239	1.874	0.3593	371.5
Octane	0.1142	2.229	2.191	1.824	0.3589	398.7
JP-8	0.1533	2252	NA	NA	0.2850	456
CO_2	0.04401	NA	NA	8.941	NA	NA
H_2O	0.01802	NA	NA	13.42	NA	NA
O_2	0.03200	NA	NA	0	NA	NA

Since JP-8 is distilled from crude oil it is not a "pure" substance, and its properties are not as well defined. The values needed were, therefore, amalgamated from a multitude of sources. The results, where appropriate, are also presented in Table 4. The molecular formula of JP-8 was approximated as $C_{11}H_{21}$,[47,48] from which the molar mass was estimated to be M = 15.33 kg/mol. NIST gives the vapor rising temperature of JP-8 to be 182.8 C°, and this is considered to be the initial boiling temperature.[49] The boiling temperature was therefore estimated as T_b = 456 K. The specific heat of liquid JP-8 can be approximated from its temperature as the following[49]:

$$c_p(\mathrm{T}) = (2.193 \pm 0.0055) + (3.996 \pm 0.0011) \times 10^{-3}(\mathrm{T} - 363.15). \quad (4)$$

Using Eq. 4, the specific heat of JP-8 was evaluated at $0.5(T_b + T_\infty)$ = 378 K, and found to be $c_{p,liq}$ = 2252 J/(kg·K). Using data from the Defense Technical Information Center,[50] the heat of vaporization for JP-8 at T = 456 K was estimated to be $h_v = (2.85 \pm 0.25)10^5$ J/kg.

Assuming complete combustion in air at stoichiometric conditions, as shown in Eq. 5, the mass ratio of oxygen to fuel (r), latent heat of vaporization (L), and heat of combustion per unit mass (Δh_c) were calculated as follows:

$$\mathrm{C_xH_y} + \left(\mathrm{x} + \frac{\mathrm{y}}{4}\right)(3.76\mathrm{N_2} + \mathrm{O_2}) \rightarrow \mathrm{xCO_2} + \frac{\mathrm{y}}{2}\mathrm{H_2O} + \left(\mathrm{x} + \frac{\mathrm{y}}{4}\right)3.76\mathrm{N_2} \quad (5)$$

$$\mathrm{r} = \frac{\left(\mathrm{x}+\frac{\mathrm{y}}{4}\right)\mathrm{M_{O_2}}}{\mathrm{M_{C_xH_y}}} \quad (6)$$

$$\mathrm{L} = \mathrm{h_v} + \mathrm{c_{p,liq}}(\mathrm{T_b} - \mathrm{T_\infty}) \quad (7)$$

$$\Delta\mathrm{h_c} = \mathrm{x}\Delta\mathrm{h}^\circ_{\mathrm{f,CO_2}}\frac{\mathrm{M_{CO_2}}}{\mathrm{M_{C_xH_y}}} + \frac{\mathrm{y}}{2}\Delta\mathrm{h}^\circ_{\mathrm{f,H_2O}}\frac{\mathrm{M_{H_2O}}}{\mathrm{M_{C_xH_y}}} - \Delta\mathrm{h}^\circ_{\mathrm{f,C_xH_y}}. \quad (8)$$

It was assumed that T_∞ = 298 K in Eq. 7 and that water remained in a gaseous state in Eq. 8. For JP-8, the value of Δh_c is given by multiple sources as Δh_c = 42.8 MJ/kg.[48,50–52]

Air properties were interpolated from data presented by Turns in *An Introduction to Combustion*.[18] For each fuel tested, the heat capacity of air was evaluated at $0.5(T_b + T_\infty)$; while, the kinematic viscosity (ν) and Prandtl number (Pr) of air were evaluated at T_b. The results are presented in Table 5.

Table 5 Selected properties of air for different fuels

Fuel	T_b (K)	$c_{p,air}$ (kJ/kg·K)	$\nu \times 10^{-5}$ (m^2/s)	Pr
Pentane	309.2	1.007	1.68	0.706
Hexane	341.9	1.008	2.01	0.701
Heptane	371.5	1.008	2.33	0.696
Octane	398.7	1.009	2.63	0.690
JP-8	456	1.012	3.16	0.686

Using the data in Tables 4 and 5 and the formulas in Eqs. 5 to 8, the values of the B-Mass Transfer Number were calculated and the results are summarized in Table 6. The calculated values of B agreed reasonably well with values presented in other sources.[16,50,53]

Table 6 Calculated fuel properties

Fuel	r	L (MJ/kg)	Δh_c (MJ/kg)	B
Pentane	3.55	0.3933	45.35	7.54
Hexane	3.53	0.4593	45.10	6.39
Heptane	3.51	0.5241	44.92	5.54
Octane	3.50	0.5835	44.79	4.93
JP-8	3.40	0.6210	42.80	4.30

5.5.1.2 Nusselt Number Correlation

Nusselt Number correlations are based on the assumption that convective heat transfer in a boundary layer scales with momentum transfer.[54,55] Nusselt Number correlations are not well studied for oscillating flows.[56] It is necessary to characterize the ratio of convective to conductive heat transfer at the wick's surface. It was assumed that the local Nusselt number at the flame position (Nu_ξ) was a function of the Reynolds Number (Re) and Prandtl Number. Using the analogy of a non-oscillating flow over a flat plate, the form was assumed as the following[54,55]:

$$Nu_\xi = cRe^{\gamma}Pr^{\delta}, \tag{9}$$

where c, γ, and δ are determined empirically.

However, the Reynolds Number calculation requires a characteristic length (ℓ). Since U_A is an rms flow velocity, ℓ was defined as the rms displacement distance of a particle in an acoustic cycle, and calculated as the following:

$$\ell = \frac{U_A}{\omega}. \tag{10}$$

Therefore, the Reynolds Number was calculated as

$$Re_A = \frac{U_A \ell}{\nu} = \frac{U_A^2}{\nu\omega}. \tag{11}$$

The Prandtl Numbers were previous evaluated at T_b and are presented in Table 5. Since c is a constant Pr is approximately constant for this project, Eq. 9 was rewritten as

$$Nu_\xi = CRe_A^\gamma, \tag{12}$$

where $C = cPr^\delta$. If $Nu' = Nu_\xi / C$ then Eq. 12 can be simplified as

$$Nu' = Re_A^\gamma \tag{13}$$

Equation 13 can be substituted into Eq. 2 to yield

$$\Theta_A' = \frac{Re_A^\gamma}{B}. \tag{14}$$

The value of γ in Eq. 14 was chosen to optimize the results of Θ_A', by minimizing the coefficient of variation. The results from this optimization are shown in Fig. 7, and the minimum occurred at $\gamma = 1/3$.

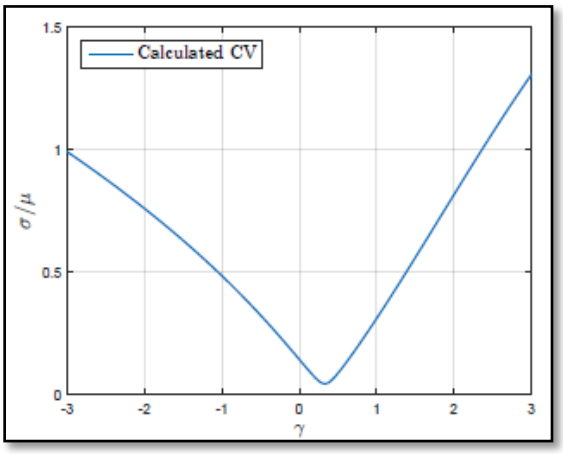

Fig. 7 Coefficient of variation for Θ_A'

Θ_A' then becomes

$$\Theta_A' = \frac{Re_A^{1/3}}{B} = \frac{U_A^{2/3}}{(\nu\omega)^{1/3}B}. \tag{15}$$

Applying the model described by Eq. 15 to the acoustic extinction data set yields highly consistent results with the average $\Theta_{Aext}' = 1.45$, Fig. 8. When the scatter in Θ_A' compared to U_{Aext} and P_{Aext}, Θ_{Aext}' is a more consistent descriptor of conditions

at extinction than U_{Aext} and P_{Aext}. Furthermore, since Θ_{Aext}' was calculated from conditions created by the lowest speaker power that could consistently cause extinction, it is proposed that Θ_{Aext}' constitutes a critical value, below which the flame continues to burn and above which total flame extinction occurs.

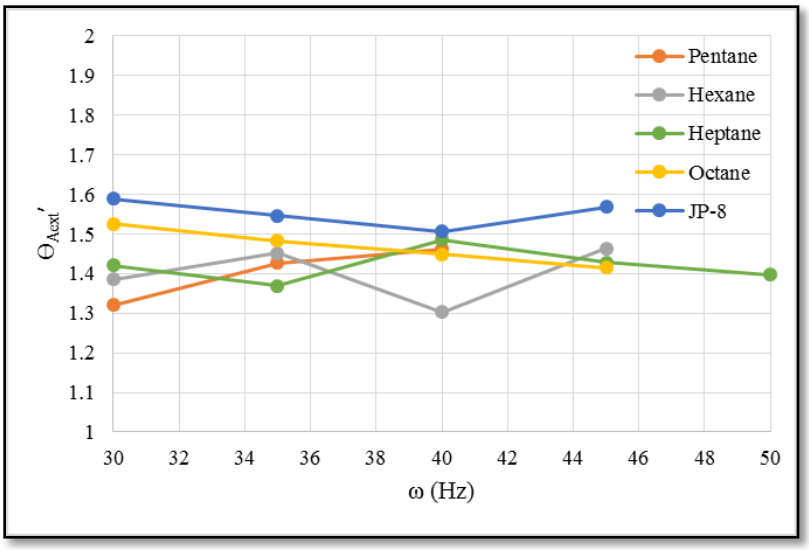

Fig. 8 Calculated Θ_A' for acoustic extinction

To test whether the Θ_{Aext}' constitutes a critical value for predicting extinction, values of Θ_A' had to be calculated for conditions above and below the minimum speaker power required to cause flame extinction. Within the total data set, there existed data was at acoustic conditions other than the minimum required to cause extinction. From these data points, values of Θ_A' could be calculated using Eq. 15. The extinction results from these trials, along with the calculated values of Θ_A' are presented in Table 7. As seen in the data, Θ_{Aext}' can constitute a critical value for predicting acoustic flame extinction.

Table 7 Analysis of hypo and hyper critical extinction conditions

Fuel	ω (Hz)	U_A (m/s)	Extinction	Θ_A'
Pentane	30	0.61	No	1.2
Hexane	30	0.52	No	1.2
Hexane	35	0.69	No	1.38
Heptane	30	0.48	No	1.25
Heptane	35	0.53	No	1.26
Heptane	45	0.69	No	1.38
Octane	30	0.50	No	1.38
JP-8	35	0.46	No	1.34
Pentane	30	0.77	Yes	1.41
Heptane	45	0.86	Yes	1.60
Heptane	50	0.78	Yes	1.45
JP-8	40	0.64	Yes	1.60

6. Acoustic Fire Suppression Prototype

Researchers from the UTD NanoTech Institute designed and fabricated 4 prototype thermoacoustic speakers for this project. The prototypes used the latest research in CNT-film thermoacoustic speakers, to develop prototypes with the potential to produce over 100-dB SPL below 100 Hz. The prototypes used 3 different designs: Panel A and B were CNT films encapsulated in 2 plates with edge activation, Panel C was CNT films encapsulated edges of a single plate, and Panel D was a CNT film encapsulated at the center of a single plate with a heat sink (Fig. 9). The thermoacoustic speakers were powered by a signal generator with amplifier, attached to the electrode leads. Prior to prototype flame-extinction tests, a sine wave sweep was performed to characterize the panel (Fig. 10). During the characterization Panels B and D were damaged due to internal arcing across the CNT array. Panels A and C were found to have insufficient SPLs below 100 Hz.

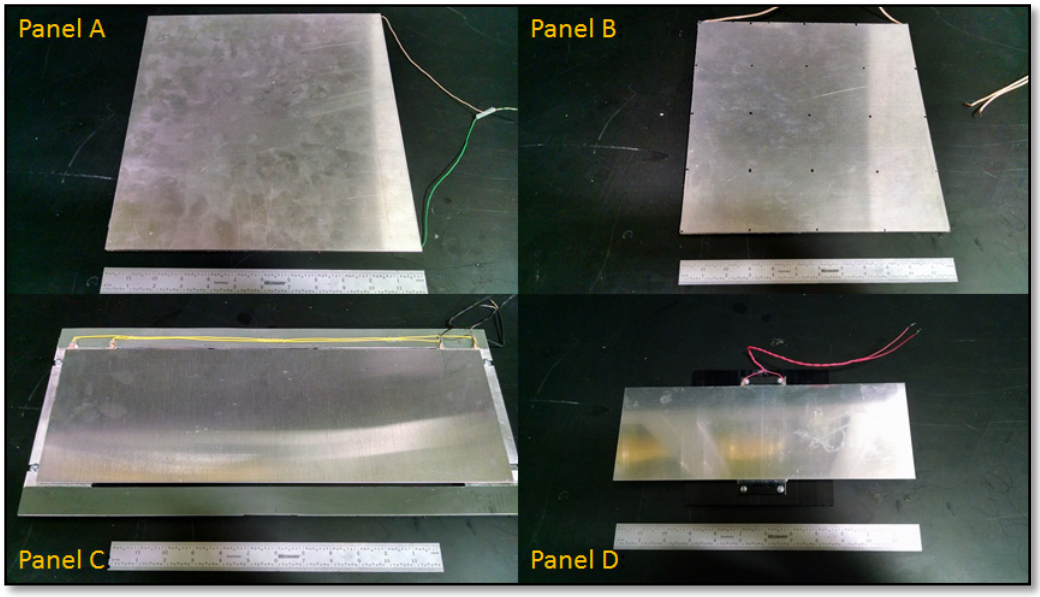

Fig. 9 Thin-film CNT thermoacoustic speaker prototypes

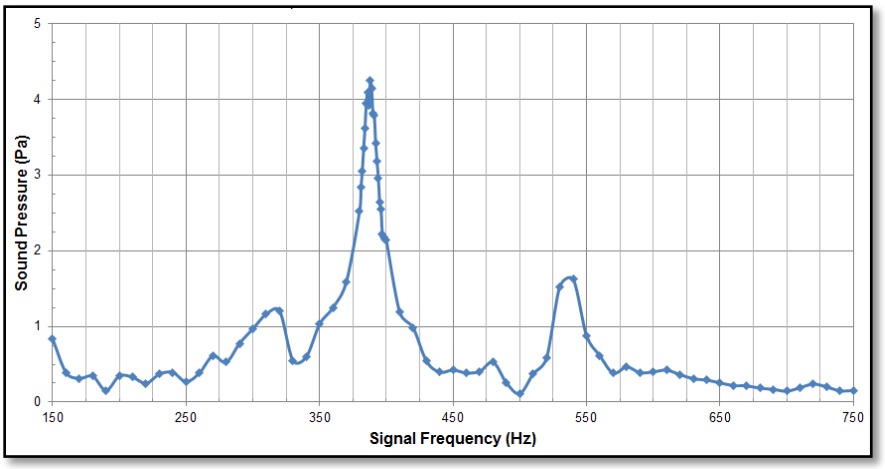

Fig. 10 Sample frequency characterization of Panel A

7. Conclusions

A study of acoustically driven extinction was carried out using the alkanes and JP-8. Samples were ignited and then subjected to acoustic perturbations at various frequencies and speaker powers until the minimum speaker power was found that could cause 3 consecutive flame extinctions. The rms acoustic pressure and air speeds were measured during each trial and, along with frequency, these measurements were used to characterize the acoustic conditions. The minimum fan-driven flows required to cause extinction for each fuel was also evaluated. Analysis of the data showed that the fan-driven air speed required to cause extinction of each fuel increased with the fuel's heat of combustion per unit mole, and that this trend was consistent with extinction strain rate theory. Using acoustics, the rms air speed at extinction was seen to decrease, which indicated that flame elongation was not the cause of extinction using acoustics. High-speed video showed that during acoustic excitation, the flame would become detached, forced away from the fuel bed, and then returned and reattached until the next cycle. It was theorized that during this displacement phase the fuel bed experienced convective cooling, and that this eventually caused the fuel's mass flux to fall below the critical amount needed to sustain the flame. This hypothesis was consistent with other theories that explain the acoustically driven extinction of droplet flames. To explore this hypothesis, the flame was conceptualized in a simple model between flame and fuel source. In this model, the Spalding B Number was used to characterize the interactions between the flame and fuel, and a Nusselt Number was used to characterize the convective cooling of the fuel bed. Mathematical expressions were then developed for each of the numbers and they were evaluated using values reported in the literature and conditions measured during the experiment. It was

found that at the minimum speaker power required to cause extinction, the ratio of the Nusselt Number to B Number was a constant for all fuels at all frequencies tested. It was found that when this ratio was below the constant, the flame continued to burn. If the ratio was greater than or equal to the constant, then flame extinction occurred. It was therefore asserted that this constant constituted a boundary between regions of flammability and flame extinction.

These data were then used to design criteria for a prototype CNT thermoacoustic speaker. Of the 3 designed and fabricated, none of the CNT thermoacoustic speakers were capable of producing over 100-dB SPL below 100 Hz. As a result none of the CNT thermoacoustic speakers were sufficient for acoustic fire extinction. Additional research and development with CNT thermoacoustic speakers is required before the technology is suitable for acoustic flame extinction at low frequencies.

8. Limitations and Considerations

According to the model developed, acoustic flame extinction requires the oscillatory movement of air to be sufficiently fast that convective cooling prevents enough fuel from being liberated to sustain the flame. Although heat transfer in a pool fire of this size is dominated by radiation,[16,18,57] for the purposes of scaling it was assumed that convection was still the primary mode of heat transfer. Another key consideration to explore though is the observation of McKinney and Dunn-Rankin,[22] who found that acoustic extinction of droplet flames required the flame to be displaced by at least the droplet's radius. Given these considerations, acoustics alone are unlikely to be suitable for controlling larger fires. However, this should not preclude development of the technology. Even if flame extinction cannot be achieved with acoustics alone, acoustics can certainly be used to destabilize the flame and even force it to become detached. If the acoustics were coupled with a known suppressing agent (e.g., water mist, dry-chemical, carbon dioxide), the combination of flame destabilization, increased mixing, and delivery of the agent directly to the fuel bed could prove to be an efficient means of fire suppression.

9. References

1. DiNenno PJ, Taylor GM. Halon and halon replacement agents and systems. In: Cote AE. editor. Fire protection handbook. Twentieth ed. Quincy (MA): National Fire Protection Association; 2008. p. 17.93–17.121.

2. McCormick S, Clauson M, Cross H. US Army ground vehicle crew compartment halon replacement program. In halon options technical working conference. 2000 May. p. 229–236.

3. Gagnon RM. Design of special hazard and fire alarm systems. 2nd ed. Clifton Park (NY): Thomson Delmar Learning; 2008. p. 10.

4. Williams FA. Combustion theory. 2nd ed. Menlon Park (CA): Benjamin/Cummings Publishing Company; 1985.

5. Quintiere JG, Rangwala AS. A theory for flame extinction based on flame temperature. Fire and materials. 2004;28:387–402.

6. Jin Y, Shaw BD. Computational modeling of n-heptane droplet combustion in air-diluent environments under reduced-gravity. International Journal of Heat and Mass Transfer. 2010;53(25-26):5782–5791.

7. Yu HZ, Newman JS. Theories of fire extinguishment. In: Cote AE. editor. Fire protection handbook. Twentieth ed. Quincy (MA): National Fire Protection Association; 2008. p. 2.80–2.92.

8. Won SH, Dooley S, Dryer FL, Ju Y. A radical index for the determination of the chemical kinetic contribution to diffusion flame extinction of large hydrocarbon fuels. Combustion and Flame. 2012;159(4):541–551.

9. Kreith F, Berger SA, Churchill SW, Tullis JP, White FM, McDonald AT, Kumar A, Chen JC, Irvine TF, Capobianchi M, Kennedy FE, Booser ER, Wilcock DF, Boehm RF, Reitz RD, Sherif SA, Bhushan B. Fluid mechanics. In: Kreith F. editor. Mechanical engineering handbook. Boca Raton (FL): CRC Press; 1999.

10. Kuo KK, Acharya R. Fundamentals of turbulent and multiphase combustion. Hoboken (NJ): John Wiley & Sons; 2012.

11. Jenkins KW, Klein M, Chakraborty N, Cant RS. Effects of strain rate and curvature on the propagation of a spherical flame kernel in the thin-reaction-zones regime. Combustion and Flame. 2006;145:415–434.

12. Candel SM; Poinsot TJ. Flame stretch and the balance equation for the flame area. Combustion Science and Technology. 1990;70(1–3):1–15.

13. Liñán A. The asymptotic structure of counterflow diffusion flames for large activation energies. Acta Astronautica. 1974;1:1007–1039.

14. Karlovitz B, Denniston DW, Knapschaefer DH, Wells FE. Fourth symposium (international) on combustion studies on turbulent flames. Symposium (international) on combustion. 1953;4(1):613–620. ISSN 0082-0784.

15. Katta VR, Meyer TR, Brown MS, Gord JR, Roquemore WM. Extinction criterion for unsteady, opposing-jet diffusion flames. Combustion and Flame. 2004;137(1–2):198–221. ISSN 0010-2180.

16. Quintiere JG. Fundamentals of fire phenomena. West Sussex (England): John Wiley & Sons; 2006.

17. Lecoustre VR, Narayanan P, Baum HR, Trouve A. Local extinction of diffusion flames in fires. Proceedings of the Tenth International Symposium on Fire Safety Science, 2011. p. 583–596.

18. Turns SR. An introduction to combustion. 3rd ed. New York (NY): McGraw-Hill; 2007.

19. McAllister S, Chen JY, Fernandez-Pello AC. Fundamentals of combustion processes. New York (NY): Springer; 2011.

20. Kim JS, Williams FA. Contribution of strained diffusion flames to acoustic pressure response. Combustion and Flame. 1994;98:279–299.

21. Whiteside GM. DARPA Instant flame suppression. Technical report. Department of Defense (US); 2013.

22. McKinney DJ, Dunn-Rankin D. Acoustically driven extinction in a droplet stream flame. Combustion Science and Technology. 2000;161:24–48.

23. Sevilla-Esparza CI, Wegener JL, Teshome S, Rodriguez JI, Smith OI, Karagozian AR. Droplet combustion in the presence of acoustic excitation. Combustion and Flame. 2014;161:1604–1619.

24. Kim SK, Choi HS, Kim HJ, Ko YS, Sohn CH. Finite element analysis for acoustic characteristics of combustion stabilization devices. Aerospace Science and Technology. 2015;42:229–240. ISSN 1270-9638.

25. O'Connor J, Acharya V, Lieuwen T. Transverse combustion instabilities: acoustic, fluid mechanic, and flame processes. Progress in Energy and Combustion Science. 2015;49:1–39. ISSN 0360-1285.

26. Miglani A, Basu S, Kumar R. Suppression of instabilities in burning droplets using preferential acoustic perturbations. Combustion and Flame. 2014;161(12):3181–3190. ISSN 0010-2180.

27. Wang HY, Bechtold JK Law CK. Forced oscillations in diffusion flames near diffusive-thermal resonance. International Journal of Heat and Mass Transfer. 2008;51:630-639.

28. Kartheekeyan S, Chakvarthy SR. An experimental investigation of an acoustically excited laminar premixed flame. Combustion and Flame. 2006;146:513–529.

29. Wang Q, Huang HW, Tang HJ, Zhu M, Zhang Y. Nonlinear response of buoyant diffusion flame under acoustic excitation. Fuel. 2013;103:364–372.

30. Hardalupas Y, Selbach A. Imposed oscillations and non-premixed flames. Progress in Energy and Combustion Science. 2002;28:75–104.

31. Deng K, Shen Z, Wang M, Hu Y, Zhong YJ. Acoustic excitation effect on {NO} reduction in a laminar methane-air flame. Energy Procedia. 2014;61:2890–2893. ISSN 1876-6102. International Conference on Applied Energy (ICAE2014).

32. Chen LW, Wang Q, Zhang Y. Flow characteristics of diffusion flame under non-resonant acoustic excitation. Experimental Thermal and Fluid Science. 2013;45:227–233.

33. Chen L-W. Application of PIV measurement techniques to study the characteristics of flame-acoustic wave interactions. Flow Measurement and Instrumentation. 2015;45:308–317. ISSN 0955-5986.

34. Nicoud F, Poinsot T. Thermoacoustic instabilities: Should the Rayleigh criterion be extended to include entropy changes? Combustion and Flame. 2005;142:153–159.

35. Nair S. Acoustic characterization of flame blowout phenomenon [PhD thesis]. [Atlanta (GA)]: Georgia Institute of Technology, School of Aerospace Technology, 2006 May.

36. Xiao L, Chen Z, Feng C, Liu L, Bai ZQ, Wang Y, Fan S. Flexible, stretchable, transparent carbon nanotube thin film loudspeakers. Nano Letters. 2008;8(12):4539–4545.

37. Aliev AE, Lima MD, Fang S, Baughman RH. Underwater sound generation using carbon nanotube projectors. Nano Letters. 2013;10(7):2374–2380.

38. Vesterinen V, Niskanen AO, Hassel J, Helisto P. Fundamental efficiency of nanothermophones: modeling and experiments. Nano Letters. 2010;10(12):5020–5024.

39. Aliev AE, Gartstein YN, Baughman RH. Increasing the efficiency of thermoacoustic carbon nanotube sound projectors. Nanotechnology. 2013;24(23):235501.

40. Hu L, Liu S, Xu Y, Li D. A wind tunnel experimental study on burning rate enhancement behavior of gasoline pool fires by cross air flow. Combustion and Flame. 2011;158(3):586–591. ISSN 0010-2180.

41. Emmons HW. The film combustion of liquid fuel. ZAAM -Journal of Applied Mathematics and Mechanics. 1956;36:60–71.

42. Raghavan V, Rangwala AS, Torero JL. Laminar flame propagation on a horizontal fuel surface: verification of classical Emmons solution. Combustion Theory and Modelling. 2009;13(1):121–141.

43. Rashbash DJ. A flame extinction criterion for fire spread. Combustion and Flame. 1976;26:411–412.

44. Tewarson A. Generation of heat and chemical compounds in fires. SFPE Handbook. 3rd ed. Quincy (MA): National Fire Protection Association; 2002.

45. Hu L, Liu S, Wu L. Flame radiation feedback to fuel surface in medium ethanol and heptane pool fires with cross air flow. Combustion and Flame. 2013;160(2):295–306.

46. NIST Chemistry WebBook. [accessed 2015 Jul 12]. http://webbook.nist.gov /chemistry/.

47. Arnold R, Anderson WE. Droplet burning jp-8/silica gels. 48th AIAA Aerospace Sciences Meeting. 2010;48(421).

48. Edwards T, Harrison B, Maurice L. Properties and usage of air force fuel: Jp-8. 39th Aerospace Sciences Meeting and Exhibit. AIAA 2001. Volume 39 of Aerospace Sciences Meeting. American Institute of Aeronautics and Astronautics, 2001 Aug.

49. Bruno TJ, Huber M, Laesecke A, Lemmon E, McLinden M, Outcalt SL, Perkins R, Smith BL, Widegren JA. Thermodynamic, transport, and chemical properties of “reference” JP-8. Gaithersburg (MD): National Institute of Standards and Technology; 2010 Jul. Report No.: NISTIR 6659.

50. The Council. Handbook of aviation fuel properties. Alexandria (VA): Coordination Research Council; 1983. Report No: CRC 530.

51. Exxon Mobile. World jet fuel specification. Leatherhead (UK): Exxon Mobile; 2005.

52. MIL-DTL-83133E. Detail specification; turbine fuels, aviation, kerosene types, NATO f-34 (jp-8), NATO f-35, and jp-8+100. Washington (DC): Department of Defense (US); 2005.

53. Spalding DB. The combustion of liquid fuels. Proceedings 4th International Symposium on Combustion, 1953. p. 847–864.

54. Incropera FP, Dewitt D, Bergman TL, Lavine AS. Fundamentals of heat and mass transfer. 6 ed. Danvers (MA): John Wiley and Sons; 2007.

55. Miles AF. Basic heat and mass transfer. Chicago (IL): Irwin, Inc., 1995.

56. Brady JF. Nusselt numbers of laminar, oscillating flows in stacks and regenerators with pores of arbitrary cross-sectional geometry. Journal of the Acoustical Society of America. 2013;133(4):2004–2013.

57. Karlsson B, Quintiere J. Enclosure fire dynamics. Boca Raton (FL): CRC Press; 2000.

List of Symbols, Abbreviations, and Acronyms

ARL	US Army Research Laboratory
CNT	carbon nanotube
DOD	Department of Defense
JASP	Joint Aircraft Survivability Program
JLF	Joint Live Fire
NIST	National Institute of Standards and Technology
rms	root-mean-square
SPL	sound pressure level
UTD	University of Texas at Dallas
VTD	Vehicle Technology Directorate

1 (PDF) DEFENSE TECHNICAL INFORMATION CTR DTIC OCA

2 (PDF) DIRECTOR US ARMY RESEARCH LAB RDRL CIO L IMAL HRA MAIL & RECORDS MGMT

1 (PDF) GOVT PRINTG OFC A MALHOTRA

1 (PDF) DIR USARL RDRL VTM B MILLS